Cite as: Jingchao Jiang, Yi Xiong, Zhiyuan Zhang, David Rosen, "Machine learning integrated design for additive manufacturing", Journal of Intelligent Manufacturing, 2020.

DOI: 10.1007/s10845-020-01715-6

Machine learning integrated design for additive manufacturing

Jingchao Jiang[1], Yi Xiong[1], Zhiyuan Zhang[1], David Rosen[1,2,*]

Abstract

For improving manufacturing efficiency and minimizing costs, design for additive manufacturing (AM) has been accordingly proposed. The existing design for AM methods are mainly surrogate model based. Due to the increasingly available data nowadays, machine learning (ML) has been applied to medical diagnosis, image processing, prediction, classification, learning association, etc. A variety of studies have also been carried out to use machine learning for optimizing the process parameters of AM with corresponding objectives. In this paper, a ML integrated design for AM framework is proposed, which takes advantage of ML that can learn the complex relationships between the design and performance spaces. Furthermore, the primary advantage of ML over other surrogate modelling methods is the capability to model input-output relationships in both directions. That is, a deep neural network can model property-structure relationships, given structure-property input-output data. A case study was carried out to demonstrate the effectiveness of using ML to design a customized ankle brace that has a tunable mechanical performance with tailored stiffness.

Keywords: Additive manufacturing; Design for AM; Machine learning.

1 Introduction

Additive Manufacturing (AM) fabricates products from digital 3D models in a piece-by-piece, line-by-line or layer-by-layer manner, which is different from conventional manufacturing processes (Jiang et al. 2019; Jiang, Xu, and Jonathan Stringer 2019; Jiang, Xu, and Stringer 2019a; Wei et al. 2020; J. Xiong et al. 2020). This gives AM more freedom on design as AM can fabricate more complicated parts, theoretically in any shape, without spending more efforts on manufacturing processes. AM bonds, places, and/or transforms volumetric primitives or elements (voxels) of raw material to fabricate the final products. The size and shape of each voxel and the bonding strength between voxels depend on the raw material properties, the AM machine (e.g., nozzle diameter), and the process parameters (e.g., print temperature, print speed, laser power). Therefore, design for additive manufacturing (DfAM) was proposed with the aim of designing and optimizing the product together with its manufacturing systems to increase the product's quality and performance, and to minimize the development time and cost (Gibson et al. 2010; Huang et al. 2020; Kim et al. 2019).

DfAM actually is a type of Design for Manufacturing and Assembly (DfMA) but is quite different from traditional DfMA. The unique capabilities of AM technologies make designers re-think the traditional DfMA process applied in AM as AM can fabricate complex structures that are impossible in conventional manufacturing techniques. AM also eliminates the assembly process as AM can manufacture the whole product in a single fabrication process. This leads to the new term of DfAM (Thompson et al. 2016), which considers the unique capabilities of AM and the difference between traditional manufacturing and AM techniques. Compared with traditional manufacturing processes, AM mainly has the following four unique capabilities: (1) shape complexity: as AM is a layer-by-layer process, it is possible to fabricate virtually any shape; (2) hierarchical complexity: hierarchical multiscale structures can be designed and manufactured from the microstructure through geometric mesostructure to the part-scale macrostructure; (3) material complexity: material can be processed one point/layer at a time in AM processes; and (4) functional complexity: fully functional assemblies and mechanisms can be fabricated directly in a single AM process. These capabilities also, however, bring new challenges in design search and optimization due to the increased number of design variables and their complicated interactions over multiple domains. Many studies have been carried out for accommodating all these design variables and reflecting their interactions, as discussed in (Y. Xiong et al. 2019), for example, and will not be detailed here. However, all these DfAM approaches are based on traditional surrogate models. In fact, machine learning (ML) can now

be applied for DfAM due to the increasingly available AM data and the powerful ability of ML to learn complex relationships among data. Table 1 compares the disadvantages and advantages between conventional surrogate model based DfAM and ML based DfAM.

Table 1 Advantages and disadvantages of conventional surrogate model based and ML based DfAM

	Advantages	**Disadvantages**
Conventional surrogate model based DfAM	-- No need to obtain large amount of data from experiments -- Comparatively low-cost	-- Hard to establish relationship equations and sometimes even impossible, especially for complex optimization problems where there are many design variables and their interactions are complicated and unclear -- Need to explore the design spaces of variables -- Hard/impossible to achieve reversed design
ML based DfAM	-- No need to establish complex relationship equations -- Easy to achieve reversed design -- Not limited by the complexity of the design problem	-- Require large amount of data

The definition of ML is "allowing computers to solve problems without being specifically programmed to do so" (Samuel 1959). The application of ML techniques has increased tremendously over the past years due to the availability of large amounts of data, computer technology development and the increased power of available ML tools (Zhao et al. 2017). ML has also been used in AM with different aims, including process optimization, dimensional accuracy analysis, manufacturing defect detection and material property prediction. In this paper, a comprehensive ML integrated DfAM framework is proposed to take advantage of ML. The framework is mainly based on using ML to learn process-structure-property (PSP) relationships proposed by (Rosen 2014). ML based DfAM can achieve reversed design without the need of establishing complex relationship equations since an ML-based output-input model can be constructed readily, given input-output data. Hence, property-structure relationships can be modelled directly, even though data were generated as structure-property relationships.

Furthermore, ML based models have virtually no limitations on the complexity of the design problem if enough data are available.

The main contribution of this paper is establishing a ML integrated DfAM framework and detailing the process of design from property to structure through ML. Furthermore, the primary advantage of ML over other surrogate modelling methods is the capability to model input-output relationships in both directions, which can achieve reversed design. The proposed ML integrated design approach can obtain the objective design directly through inputting the property requirements, which traditional surrogate model based design process cannot achieve. Section 2 reviews the literature on traditional surrogate model based design and the existing applications of ML in AM. Then Section 3 details the proposed ML integrated DfAM framework. Section 4 demonstrates an ankle brace case study to show the design process using ML. The last section provides conclusions.

2 Literature review

In this section, literatures related to conventional surrogate model based design and ML applications in AM are briefly reviewed.

2.1 Surrogate model based design

In conventional surrogate model based design processes, design exploration and exploitation are often adopted which are the two main strategies to provide insight into the design space. Malak et al. (2009) proposed a combined model for conceptual design, considering both multi-attribute utility theory and the perspective of set-based design. With the aim of designing heterogeneous scaffolds for tissue engineering, Weiss et al. (2005) built multi-stage Bayesian surrogate models to describe the relationship between the design parameters and the therapeutic response. Pacheco et al. (2003) proposed a covariance-based method to establish multistage surrogate models in the conceptual design stages for a thermal design problem. Bayesian network classifier (BNC) based design exploration methods were proposed by Morris et al. (2018) and Matthews et al. (2016) to design negative stiffness metamaterials with better mechanical stiffness and loss properties. In addition, Shahan and Seepersad (2012) proposed a Bayesian network classifiers model to classify the design space into unsatisfactory or satisfactory regions for designing a spring and an unmanned aerial vehicle. These BNC methods formulated relationships between design spaces in the analysis direction (e.g., structure to property), then used back-propagation to invert the relationships. Unal et al. (2017) combined model-based simulation and set-based design to obtain the design space for designing seismic-

resisting structural frames. Choi et al. (2008) developed an inductive design exploration method for designing robust multiscale materials. However, since these design approaches are surrogate model based, each requires an iterative approach to inverting an input-output relationship that is central to their design process. It is recognized that Bayesian network classifiers are often considered as a ML method.

2.2 Machine learning in design for AM

Machine learning has already been used in AM with different aims such as process optimization and manufacturing defect detection. Table 2 lists the available studies that can be seen as using ML for some DfAM considerations with corresponding objectives. They mainly focus on using ML to improve or optimize the process parameters for AM techniques with corresponding property requirements. However, they are not proposed in a systematic way for DfAM.

References (Li et al. 2019; Mahapatra and Sood 2012) used ML to predict surface roughness of AM printed parts in different process parameters in material extrusion (MEX) (informally called fused deposition modeling (FDM)), while others (W. Zhang et al. 2017) used ML to predict the surface roughness of AM fabricated Ti-6Al-4V parts in powder bed fusion. References (Lao et al. 2020) and (H. Chen and Zhao 2015) used ML to predict the surface qualities of AM fabricated parts in 3D Concrete Printing and binder jetting, respectively. The above studies can be used to design AM products with required surface quality. ML has been applied to predict geometric accuracy and dimensional variations of AM printed parts using MEX (Khanzadeh et al. 2018) (Tootooni et al. 2017) and in polymer powder bed fusion (PBF) (Baturynska et al. 2019). Several groups have applied ML to predict deposit sizes in directed energy deposition, including bead width and height in wire-arc DED (J. Xiong et al. 2014) and printed part height in laser-based DED (Lu et al. 2010). Thermal deformation of printed parts has been modeled using ML for PBF parts (Chowdhury and Anand 2016). These studies can be used to design AM products with geometric requirements. Jiang et al. (2019) used ML to predict printable bridge length in different process parameters that can be used to design support structures in AM. All the above research works can be seen as process-structure relationship studies from the viewpoint of DfAM.

Regarding mechanical and physical properties, some groups have developed process-property relationships using ML. One group (Baturynska 2019) applied ML to predict the mechanical properties of polymer powder bed fusion manufactured polyamide 2200 parts. Vijayaraghavan et al. (2015) used ML to predict wear strength of printed parts in MEX. Mohamed et al. (2017)

used ML to optimize the process parameters for obtaining required viscoelastic properties of fabricated parts in MEX. ML has also been applied in (Negi and Sharma 2016) to optimize the process parameters for obtaining required shrinkage behaviour of printed PA 3200GF specimens in PBF. These studies can be used to design AM products with mechanical requirements. However, the research focused on property prediction, not part design from a holistic DfAM viewpoint. In contrast, this paper will propose a comprehensive ML integrated DfAM framework based on process-structure-property relationships. A case study will be carried out to show the ML enabled design process from property to structure.

Table 2 Available studies on using ML for DfAM

Objectives	Reference	Machine learning technique used	Corresponding AM
Predict surface roughness of printed parts in different process parameters	(Li et al. 2019)	Random forests, AdaBoost, Support vector machine (SVM)	MEX
	(Mahapatra and Sood 2012)	Artificial neural network (ANN)	MEX
Predict geometric accuracy of printed parts	(Khanzadeh et al. 2018)	Self-organizing map, KMeans unsupervised clustering	MEX
Predict dimensional variation in MEX printed parts	(Tootooni et al. 2017)	Sparse representation, K-Nearest Neighbors, neural network, naïve Bayes, SVM, Decision tree	MEX
Predict printable bridge length	(Jiang et al. 2019)	Back propagation neural network	MEX
Predict the width and height of printed bead	(J. Xiong et al. 2014)	Neural network	Wire arc DED
Predict depositing height of printed parts	(Lu et al. 2010)	BPNN, LS-SVM	Laser DED
Predict surface roughness of printed Ti-6Al-4V parts	(W. Zhang et al. 2017)	BPNN	PBF
Predict the thermal deformation of printed parts	(Chowdhury and Anand 2016)	ANN	Laser PBF
Predict dimensional accuracy of printed parts	(Baturynska et al. 2019)	Multi-layer perceptron, Convolutional neural network (CNN)	Polymer PBF
Predict extruded surface quality	(Lao et al. 2020)	ANN	3D Concrete
Predict qualities (e.g. surface roughness) of printed parts	(H. Chen and Zhao 2015)	BPNN	Binder jetting
Predict wear strength of printed parts	(Vijayaraghavan et al. 2015)	Multi-gene genetic programming, ANN, SVM	MEX
Optimize process parameters to obtain required viscoelastic properties	(Mohamed et al. 2017)	ANN	MEX
Optimize process parameters to obtain required shrinkage behaviour of printed PA 3200GF specimens	(Negi and Sharma 2016)	ANN	PBF
Predict the mechanical properties of manufactured polyamide 2200 parts	(Baturynska 2019)	Decision Tree, Gradient Boost,	PBF

3 Machine learning integrated DfAM

3.1 Process-structure-property relationships

A design problem formulation was proposed (Rosen 2007) for computer-aided design (CAD) using the process-structure-property (PSP) linkage, as shown in Fig. 1. For example, in the MEX process, PSP relationships for polymers relate process conditions such as print temperature, to microstructure characteristics such as voids, to mechanical properties such as strength. Traditionally, PSP relationships are mainly obtained through surrogate models. However, the PSP relationships are generally highly non-linear, high-dimensional and even non-convex, which makes it hard to establish the PSP relationships with high accuracy, particularly for some complicated problems. In this paper, we propose a ML integrated framework to establish the relationships between process, structure and property as shown in Fig. 2(a). For instance, the process parameters from AM processes (e.g., print speed, print temperature, layer thickness and others) can be the inputs for ML model, while corresponding obtained structure parameters (e.g., surface roughness, dimensional accuracy, voids) can be the outputs for training the ML model. Then the trained ML model records the process-structure relationship that can be used in future design processes. Alternatively, an ML-trained model can utilize the structure parameters (e.g., surface roughness, dimensional accuracy) as the inputs while the AM process parameters (e.g., print speed, print temperature, layer thickness and others) can be the outputs for obtaining the relationship from structure to process. Thus the trained ML model can be used for future designs from structure to process. Similarly, other relationships among process-structure-property can also be established in whichever direction through ML as shown in Fig. 2(b).

In fact, the studies listed in Table 2 can be categorised into establishing the relationships of process-structure or structure-property. However, none of these studies proposed a complete framework for ML integrated DfAM based on PSP model. Fig. 2 depicts how the complex relationships between process-structure-property can be learned using ML. With the help of ML, the analysis process from process to structure then to property and the design process from property to structure then to process (as shown in Fig. 1) can now be combined with the help of ML (Fig. 2). Next, we will provide and detail a ML integrated DfAM method based on property-structure relationships.

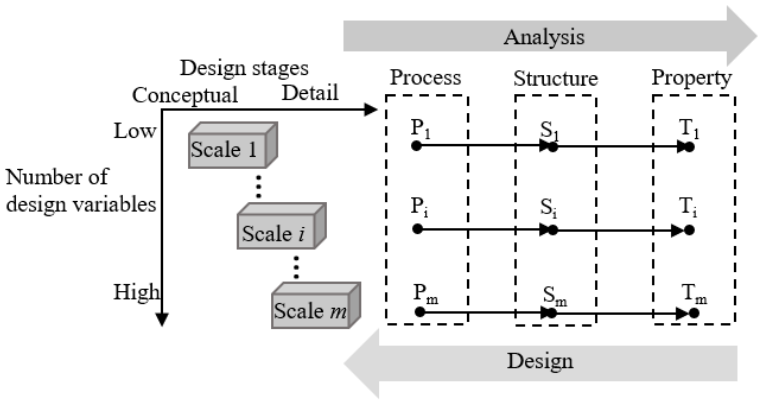

Fig. 1 Process-structure-property-based design problem formulation for DfAM proposed in (Rosen 2014)

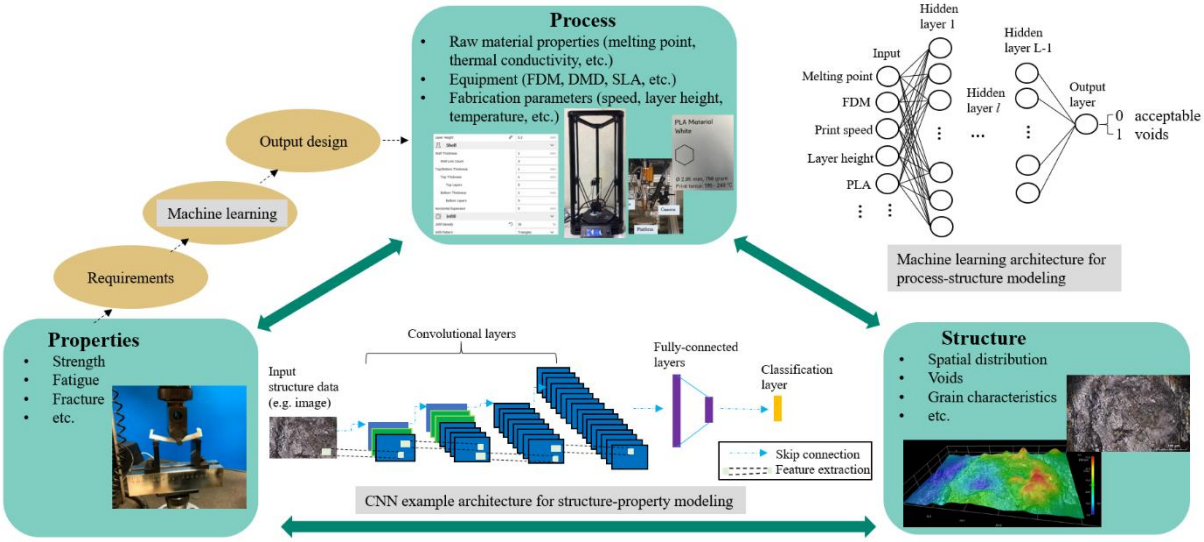

(a)

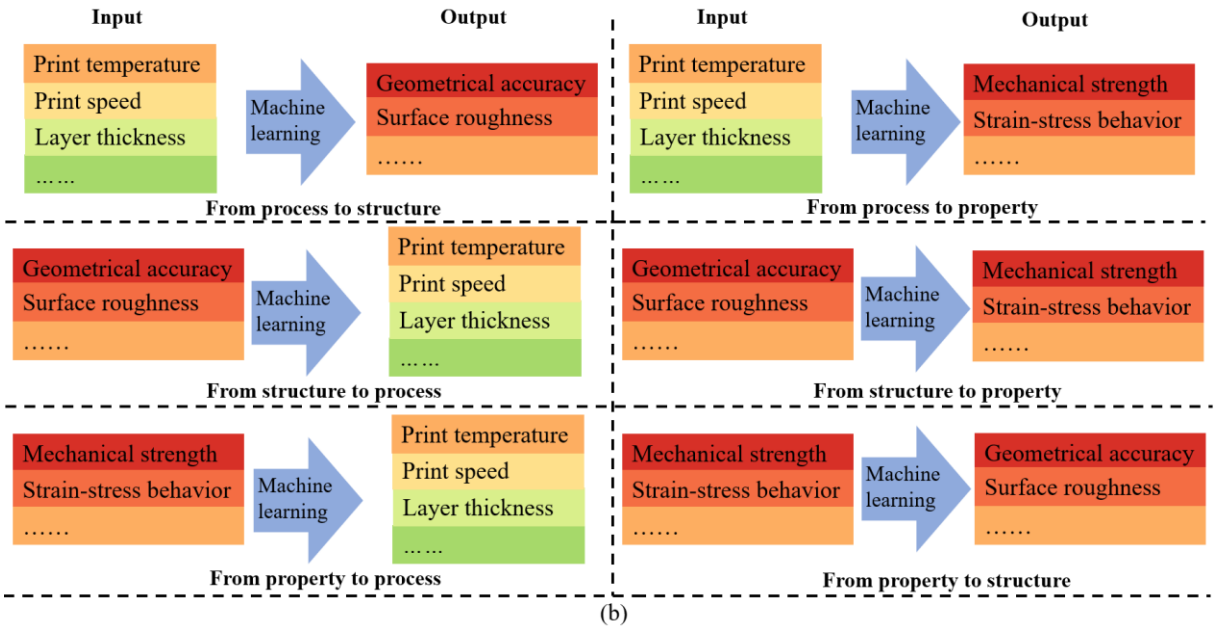

(b)

Fig. 2 Illustration of ML for PSP relationship establishment; (a) Proposed ML integrated framework for establishing process-structure-property relationships; (b) Examples of how to establish PSP relationships in whichever direction via ML

3.2 Design approach

In this section, we propose a specific ML integrated DfAM method based on property-structure relationships. This design method can be used to design products where distributions of mechanical properties are desired. The achievement of these mechanical property distributions will be achieved by tailoring part geometry, not by using multiple materials. Fig. 3 shows the framework of how this design method works. The proposed design method includes four steps.

Step 1: Determine the desired design space. This includes determining the properties/responses that are of interest (e.g., stress-strain responses of an ankle brace) and the design variables that are of interest (e.g., the geometric variables of horseshoe structure for ankle brace). Design a sampling strategy for the design space, then for each sampled point obtain the corresponding mechanical properties through simulation (e.g., ABAQUS). This will record the mechanical properties of parts in different geometries. The aim of this step is to get enough data for machine leaning model establishment.

Step 2: Establish the ML model. When choosing the basic structure of ML (e.g., convolutional neural network (CNN), deep neural network (DNN)), the following rules can be considered.

- If the requirement for the mechanical property is to represent a distribution (for example, the stress-strain response is required to be the exact curve as shown in Fig. 7(b)), then a CNN can be used to establish the model. The image of the stress-strain response, or other desired property distribution, can be used for training since CNNs are very effective in image classification and recognition (Gu et al. 2018).
- If the property requirement is only based on one or several points, rather than the entire stress-strain curve or other distribution (e.g., the stress is 10 MPa when the strain is 0.3 in orientation 1 in Fig. 7(b)), then a DNN can be used for establishing the machine learning model. The relationship between inputs and outputs with exact values can be cast as a regression problem that can be well resolved by DNNs (Liu et al. 2017).

Step 3: After the ML model is established, the required mechanical properties can be used as the input (points data for DNN, images for CNN). Then the ML model can directly output the corresponding qualified geometries of the design.

Step 4: Finally, the obtained part with designed geometries can be sent for fabrication using additive manufacturing.

A case study will be carried out in the next section to illustrate the proposed ML enabled design method in detail.

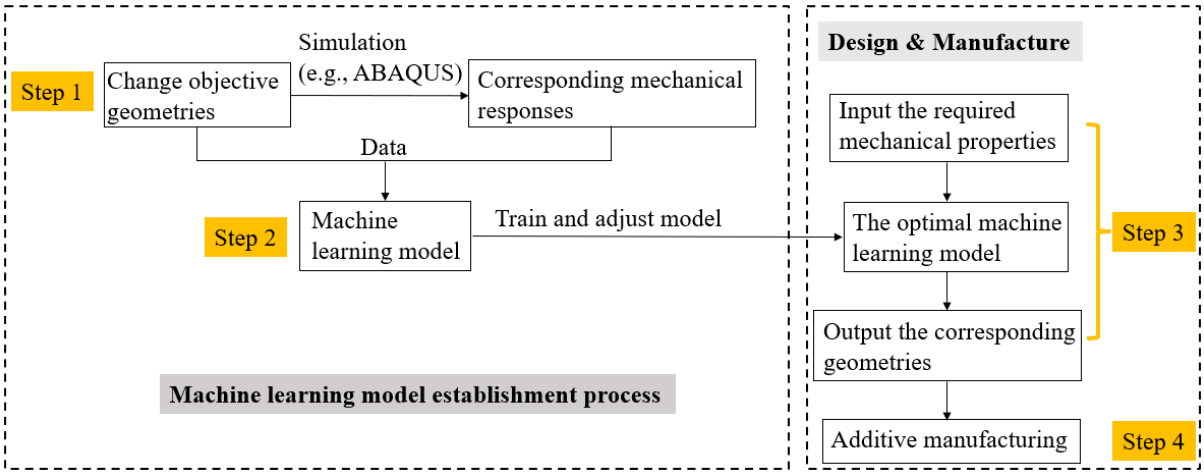

Fig. 3 Framework of the proposed design method

3.3 Machine learning model

3.3.1 Deep neural network (DNN)

A neural network usually contains layers of interconnected nodes (neurons) and links connecting the nodes to establish a network. Generally, there are three main components in a typical node of a neural network: a weighted sum of the input values ($\sum_{i=0}^{n} w_i x_i$), an activation function (g) and a bias (b) as shown in Fig. 4(a). The input values (x_i) in each node from previous connected nodes are multiplied with a weight (w_i), and then summed. The weighted sum is then added by a bias (b) to control how easily a node is activated. This value is then passed to an activation function (e.g., softmax, Sigmoid or ReLU), gaining the final output value (y) of the node. This process can be expressed as Equation 1. The biases (b) and weights (w_i) are DNN parameters that can be learned and tuned automatically during the training process.

$$y = g(\sum_{i=1}^{n} w_i\, x_i + b) \tag{1}$$

A network layer comprises a number of nodes and a set of layers can form the neural network. Fig. 4(b) shows an example structure of DNN. At least three layers are needed to establish a typical neural network: an input layer, a hidden layer and an output layer. Generally, there should be only one input layer and one output layer. The number of hidden layers is determined by the size and complexity of the relationships being modeled. Once there are several hidden

layers in a neural network (rather than only one), the neural network is called deep neural network (DNN). Among the many activation functions available, the ReLU function is comparatively the most efficient and is used frequently. ReLU returns an output equal to the input for all positive input values while returning zero for all other input values, as shown in Equation 2. The advantage of ReLU is that it can reach convergence much faster than Tanh/Sigmoid and it has no vanishing gradients problem (He et al. 2015).

$$ReLU(x) = \max(x, 0) = \begin{cases} x & x > 0 \\ 0 & else \end{cases} \quad (2)$$

Generally, the following parameters can be tuned and adjusted during the DNN model establishment process: activation function, layer number, the optimizer (Adam, etc.), neuron number in each layer, batch size, dropout and normalization. In our proposed DfAM method, we suggest to use ReLU as the activation function, Adam as the optimizer, and use normalization in DNN. In terms of the layer number, it depends on the complexity of the design problem; more layers may be needed for more complex data and relationships to be learned. Generally, the more input features and/or output features, the more layers will be needed. The best number of layers needs to be determined by testing. The neuron numbers in each layer need to be determined as well. Again, complex input-output relationships require more neurons in the hidden layers. However, the number of neurons from the first layer to the last layer (layer 1 to layer 9 in Fig. 4(b)) should be increased first, reach a highest number in the middle layer, then decrease. The neuron numbers from the first layer to layer 9 in the example of Fig. 4(b) are 10, 20, 40, 60, 80, 60, 40, 20, and 10.

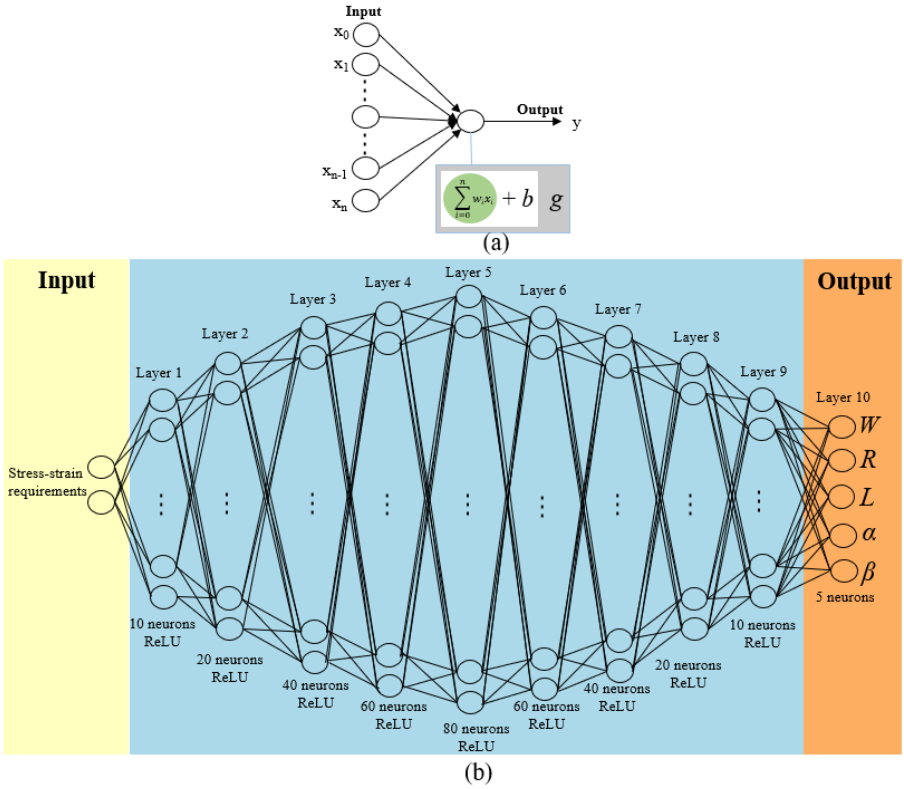

Fig. 4 Illustration of DNN; (a) working principle illustration of a typical neuron; (b) example structure of DNN

3.3.2 Convolutional neural network (CNN)

Convolutional neural networks (CNN) are a class of deep neural networks. They have the ability to analyse visual imagery such as the images of stress-strain curves) (Jin et al. 2017). CNNs employ a mathematical operation called convolution which is a specialized kind of linear operation for image analysis. CNNs are similar to general neural networks that use convolution in place of general matrix multiplication in at least one of their layers. A CNN consists of an input and an output layer, as well as multiple hidden layers, similar to any other type of neural network. Fig. 5 shows an example of using a CNN to recognize the features of stress-strain curves. As illustrated, the CNN extracts the curve features of the input image, then connects the specific curve features in each image to its corresponding part geometries. Therefore, CNNs can be used for establishing property-structure relationships used for design when the mechanical requirements are distributions.

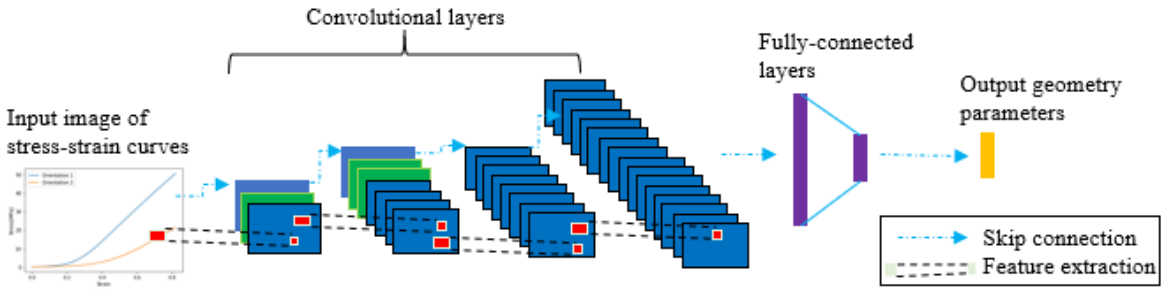

Fig. 5 Example of using CNN to recognize the features of stress-strain curves

4 Case study

In this section, the proposed ML integrated design method is applied to design an additively manufactured ankle brace that has tailored stiffness requirements. This case study exemplifies the utilization of property- structure relationships established by ML. The ankle brace is to be fabricated with a stiff polymer material by using a material jetting AM technique.

4.1 Design problem statement

When a person's ankle joint is injured (e.g., acute sprains), ankle braces generally can be used as orthoses for assisting rehabilitation. Ankle braces help to prevent further injury to the ankle joint while allowing restricted movements. The range of motions and allowable loading conditions for joints along the course of recovery can be adaptively adjusted by using the optimally designed ankle braces, ensuring tissue healing while avoiding extreme load conditions (Thiele et al. 2018). In this case study, the design of the geometric structure of the ankle brace is carried out by using ML and compared to results using a different design method and surrogate models based on Gaussian process regression [8].

Fig. 6(a) shows a 3D foot model and Fig. 6(b) shows the flattened ankle brace. The design goal is to achieve the required motion range in all three orientations, as shown in the figure, by filling the whole ankle brace with designed geometric structures. In this case study, the ankle brace was designed as a 2D geometric structure optimization problem, thus can be fabricated in additive manufacturing without support material consumption to save material wastes (Jiang et al. 2018a, 2018b; Jiang, Xu, and Stringer 2019b). Based on the studies of (J. Chen et al. 1988; Siegler et al. 1988), the typical ranges of motions during the recovery process are listed in Table 3. The design domain is further divided into three zones as shown in Fig. 6(b), based on their different contributions for limiting the range of motions in three orientations. As depicted in Fig. 6(a), the ankle joint can be considered as a ball joint that has its pivot point located at the

origin of the defined coordinate. The equilibrium of moments can then be constructed to specify design requirements for each zone. In order to simplify the analysis, only axial deformations in two orthogonal orientations are evaluated. More complex deformations can be decomposed into these two orientations. As illustrated in Fig. 6(b), the stiff and soft orientations are denoted as orientations 1 and 2, respectively. Considering the allowable strain and original geometry, the stress-strain requirements for each zone are specified as shown in Table 4 (Y. Xiong et al. 2019). In this case study, a horseshoe structure unit cell (a type of flexible lattice structure), shown in Fig. 7(a), was used as the basic design unit to tailor the stress-strain response of each zone. The horseshoe structure has a nonlinear stress-strain response and is highly stretchable (Jang et al. 2015). There are two advantages when using the horseshoe structure. Firstly, the nonlinear J-shape stress-strain response of these horseshoe structures is similar to the mechanical behaviour of biological soft tissues, requiring only small efforts to move the ankle until it reaches the maximum allowable motion range, when its stiffness increases significantly, as shown in Fig. 7(b). In addition, the anisotropic mechanical property allows different ranges of motions in two different orientations.

The stress-strain response can be tuned through designing the geometric structure of horseshoe. As displayed in Fig. 7(a), the geometric structure of horseshoe has five design variables: width *W*, radius *R*, length *L*, angle α and angle β. Once these variables are determined for meeting the motion requirements (stress-strain requirements), the designed horseshoe structure can then be fabricated by additive manufacturing.

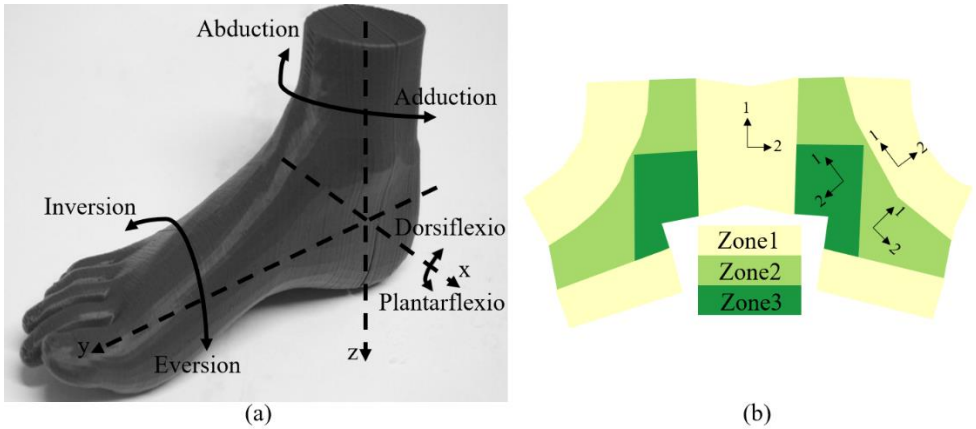

Fig. 6 (a) 3D foot model; (b) flattened ankle brace

Table 3 One set of maximum torque and range of motions for an ankle joint

	Maximum torque	Range of motion
X	20 Nm	± 20º
Y	17.5 Nm	± 5º

Z	17.5 Nm	± 5°

Table 4 Stress-strain requirements for each zone

	Orientation	Stress (MPa)	Strain
Zone 1	1	0.47	0.3
	2	0.24	0.1
Zone 2	1	0.28	0.1
	2	0.28	0.1
Zone 3	1	0.43	0.1
	2	0.49	0.1

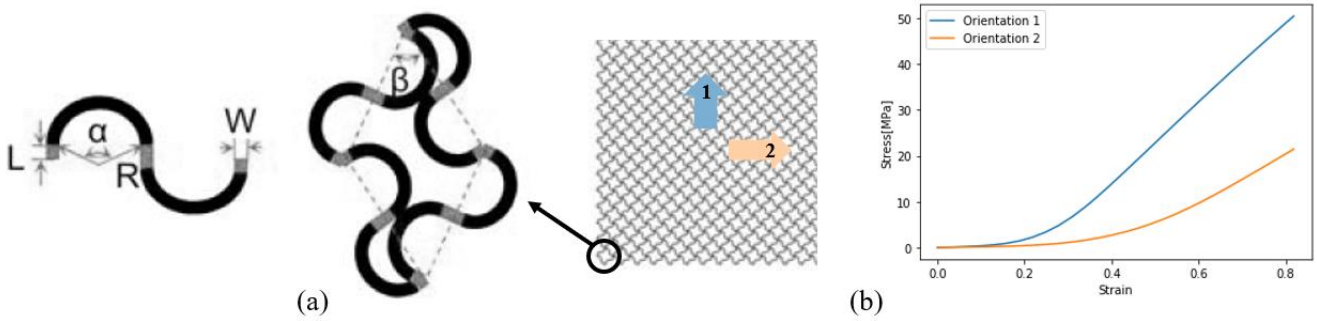

Fig. 7 (a) A quad horseshoe structure unit cell and its five design variables and (b) its stress-strain relationships

4.2 Machine learning model establishment

Before using ML to design the required geometric values (*W*, *R*, *L*, α and β) for meeting corresponding stress-strain responses, the ML model and the data for training the model should be obtained. The ranges of the design variables are listed in Table 5. Thousands of data points within the range of each variable were generated randomly and different variable values were also combined randomly to obtain different groups of values of the variables. Then, geometric models of horseshoe lattice structures representing the data point were fed into ABAQUS/STANDARD (Dassault Systèmes®, 2017) to characterize their corresponding stress-strain responses in both orientations. This study considers the in-plane deformation only, and the structure was therefore modelled as 2D beams using B32H elements. To avoid edge effects, a square matrix with a sufficiently large number of horseshoe unit cells (5 × 5) was used in the simulation. Nodes on the bottom edge of the horseshoe matrix were fixed with an encastre boundary condition; meanwhile, a tensile load was applied through a displacement control of nodes on the top edge of the horseshoe matrix.

Table 5 Ranges for design variables of a horseshoe unit cell

Design variable	Width (W)	Radius (R)	Length (L)	Angle (α)	Angle (β)
Range	0.1-0.4 mm	0.8-1.8 mm	0.1-0.2 mm	0.1-1 rad	0.1-0.5 rad

After obtaining the stress-strain responses, a property-structure model was generated by training a DNN. The stress-strain responses were the inputs while the corresponding values of the *W*, *R*, *L*, α and β variables were used as the output, as shown in the bottom arrow in Fig. 8. After the ML model was trained with sufficient accuracy, the required stress-strain response for the ankle brace can then be fed into the ML model to obtain the corresponding design geometry of horseshoe structure in terms of values of the five design variables.

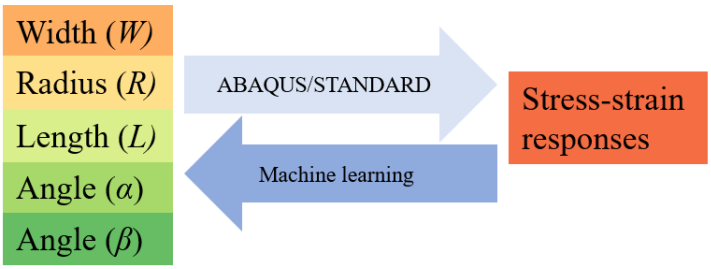

Fig. 8 Illustration of obtaining stress-strain responses using ABAQUS (top arrow) and using ML to obtain the relationship between responses and variables (bottom arrow)

A Deep Neural Network (DNN) was used to establish the ML model for this case study as the relationship between inputs and outputs can be cast as a regression problem that can be well resolved by DNN. In this case study, a deep neural network model with ten layers (as shown in Fig. 4(b)) was used to establish the relationship between the *W*, *R*, *L*, α and β variables and stress-strain responses. The corresponding numbers of neurons and activation functions used in each layer are listed at the bottom of each layer in Fig. 4(b). The number of neurons should be increased and then decreased as the layer number increases. The neuron number in the middle layer should be the largest. This is the general case and, in these settings, the machine learning model generally can work with better accuracy. In terms of the exact numbers in each layer, we tested on the numbers and determined to use these neuron numbers in each layer with the best accuracy as shown in Fig. 4(b). The activation function ReLU was used in the first 9 layers.

Next, we will illustrate the process of using ML to obtain the ankle brace design for Zone 1. Design for Zones 2 and 3 is similar to Zone 1. As can be seen from Table 4, the requirement of

stress-strain responses for Zone 1 is as follows: when the strain is 0.3, the stress should be 0.47 MPa in orientation 1; when the strain is 0.1, the stress should be 0.24 MPa in orientation 2. Therefore, 300 groups of data with stresses between 0.20 to 0.29 MPa in orientation 2 and 0.42 to 0.55 MPa in orientation 1 when strain is 0.1 were selected to train the ML model. The reason of refining the range of stress and strain is for increasing the ML model's accuracy and performance. After tuning the ML model with these data, the best ML model parameters were obtained as follows: layers, neuron number in each layer and activation functions as shown in Fig. 4(b); the number of epoch was set at 200; batch_size was set as 10; optimizer was set as "adam"; and loss and metrics were both set as "mse" (mean squared error). Among these data, 270 groups of data were used for training while the remaining 30 groups of data were used for testing the performance of the ML model. Table 6 shows the results of the ML model's performance. Similarly, ML models were also established accordingly for Zones 2 and 3. The performances on Zones 2 and 3 are also shown in Table 6. As can be seen, the ML model has satisfactory accuracy.

Table 6 Mean squared errors of established Zone 1 ML model

	Training data	Testing data
Zone 1	0.000003638	0.000002867
Zone 2	0.000009832	0.000008503
Zone 3	0.000004439	0.000005729

4.3 Results

The corresponding ankle brace design with the requirements as listed in Table 4 can be obtained now using the established ML model. For the horseshoe geometry of Zone 1, the corresponding stresses of 0.47 and 0.24 were fed into the ML model to obtain the geometric values *W, R, L*, α and β. Similarly, Zones 2 and 3 were designed using their ML models. Fig. 9 shows the corresponding inputs and design outputs for the three zones. To evaluate the real stress-strain responses of these three zones, the corresponding outputs shown in Fig. 9 were used for running simulations in ABAQUS. The real stress-strain responses using design variable values in Fig. 9 are displayed in Fig. 10. As can be seen, the stress values and corresponding strains are all close to the required values as listed in Table 4. The maximum deviations from the targets are all less than 0.05 MPa, which was deemed to be acceptable (Y. Xiong et al. 2019). Therefore, the ankle brace can be designed using the ML model outputs. All zones in the 2D structure were populated and filled with these horseshoe designs. In the adjacent areas, boundaries of different

designs were connected by joining open-ended struts to their nearest neighbours. If a unit cell is cut by a boundary, the resulting struts are connected to the neighbouring unit cell across the boundary. This guarantees a connected structure without hanging struts. It may result in slightly different properties along the boundary, but these deviations will be small. The design was then stored in STL files and fabricated using a material jetting process (Stratasys® Polyjet J750). The material used for fabrication was the Vero Cyan material, a stiff photopolymer (Poisson's ratio: around 0.5 and Young's modulus: around 1.7 GPa) from Stratasys®. Fig. 11 shows the final fabricated ankle brace that was folded to conform to the surface of the ankle.

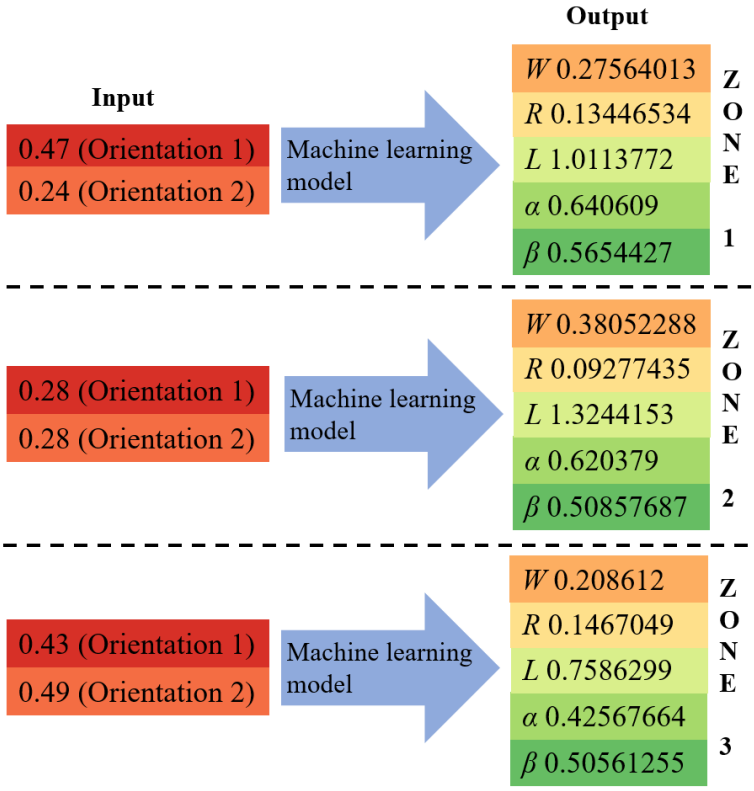

Fig. 9 Inputs and obtained design outputs of the three zones by using ML

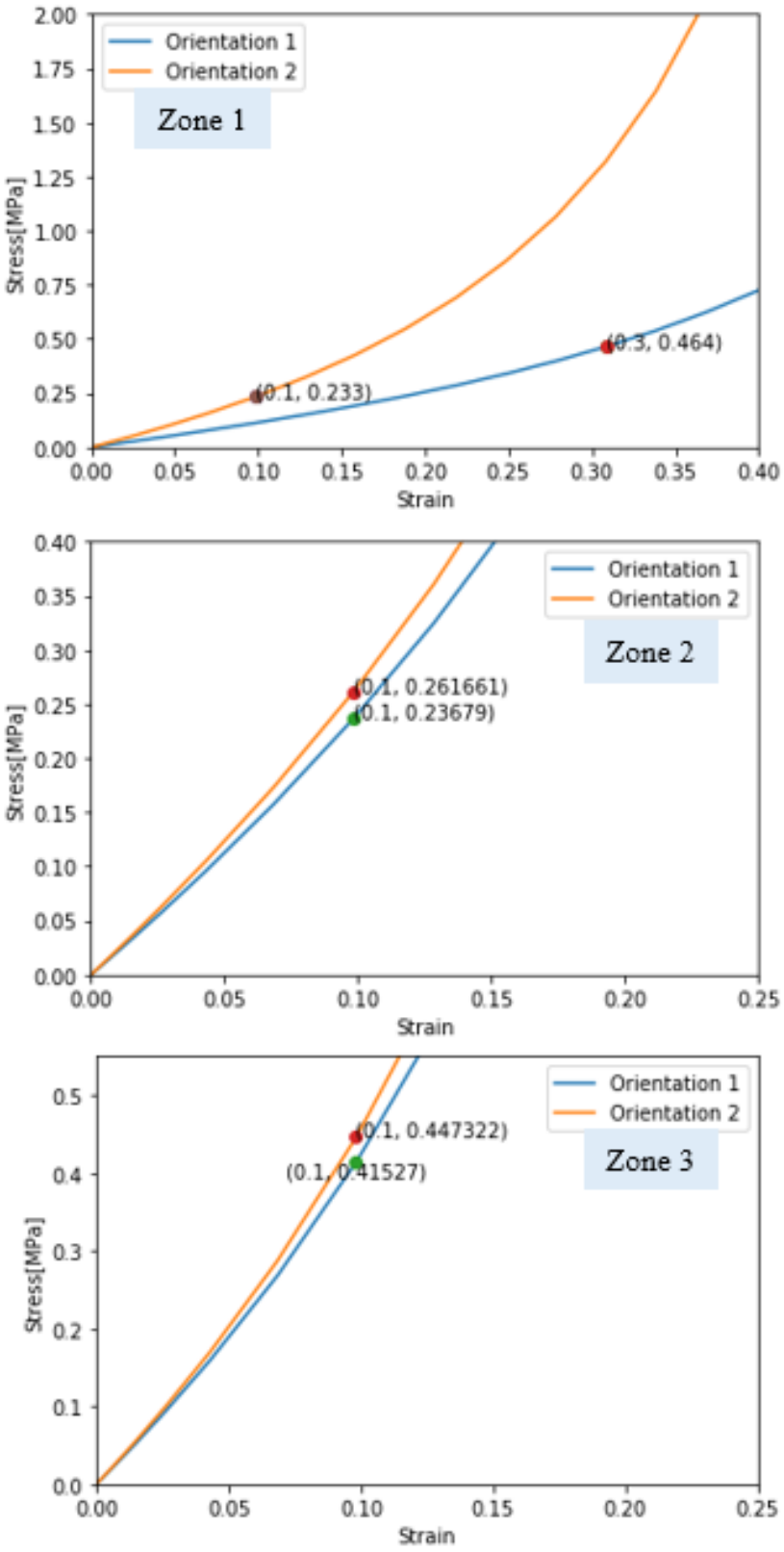

Fig. 10 Real stress-strain responses in the three zones using the ML obtained design

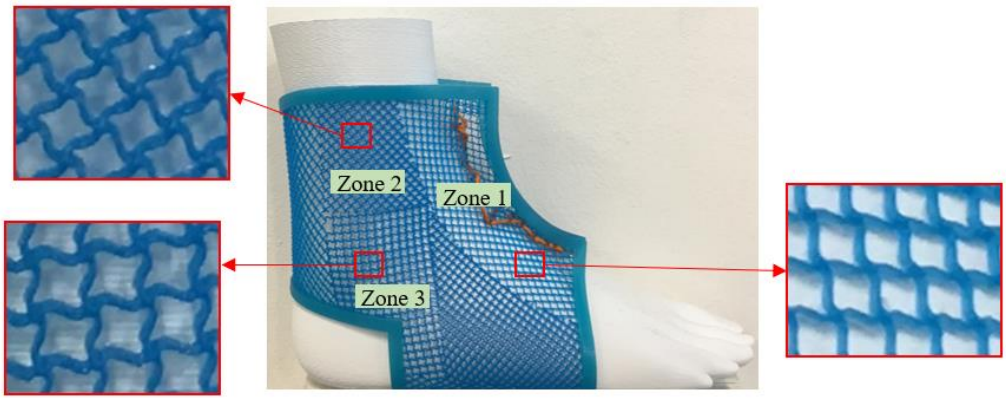

Fig. 11 Final fabricated ankle brace with close views in each zone

4.4 Discussion

The ankle brace design problem was first formulated and solved using Gaussian process regression surrogate models (Y. Xiong et al. 2019), which required the use of optimization to compute design variable values, given desired stress-strain relationships. Optimization was required since the structure-property relationship was modelled using the GPR model, and attempts to use GPR to model property-structure relationships were not successful. In this paper, we used a ML enabled design approach to solve the same problem. The primary advantage of our proposed DfAM method is the capability to model input-output relationships in both directions. That is, a deep neural network can model property-structure relationships, given structure-property input-output data, which enables the direct computation of design variable values without the need to invert the structure-property relationship. Table 7 compares the real stress and strain values obtained according to the final design in (Y. Xiong et al. 2019) and the obtained design in this paper. As can be seen, the obtained stress values from the designed brace in this paper are closer to the required values than the design in (Y. Xiong et al. 2019) in terms of orientation 1 of Zone 1 and orientation 1 of Zone 3. However, all the values are quite close and both the design from (Y. Xiong et al. 2019) and this paper are acceptable.

Table 7 Comparison between obtained stress values from designs in (Y. Xiong et al. 2019) and this paper

	Orientation	Strain	Required Stress (MPa)	Obtained stress from ML model	Relative error	Obtained stress from surrogate model (Y. Xiong et al. 2019)	Relative error
Zone 1	1	0.3	0.47	0.464	0.006	0.484	0.014
	2	0.1	0.24	0.233	0.007	0.235	0.005
	1	0.1	0.28	0.237	0.043	0.268	0.012

Zone	2	0.1	0.28	0.262	0.018	0.265	0.018
Zone	1	0.1	0.43	0.415	0.015	0.411	0.019
3	2	0.1	0.49	0.447	0.043	0.451	0.039

To illustrate the advantage of the ML based method, computation times will be considered for determining design variable values. Our ML method only takes 2ms or so to compute the design once the ML model has been established. For the conventional surrogate model in (Y. Xiong et al. 2019), it takes about 19s to get the design, about 5 orders of magnitude difference. The effectiveness of our method is based on the ability of ML to establish the process-structure-property relationship in whichever direction as shown in Fig. 2. This paper only shows the example of "from property to structure" due to the current limited data from AM. However, as additional AM data and relationships are determined, more complete and powerful PSP models can be established in the future directly through ML to support a wide range of design problems.

5 Conclusions

In this paper, a ML integrated DfAM framework is proposed to establish process-structure-property relationships, which can be helpful to design for additive manufacturing. With the help of ML, the analysis and design processes based on PSP no longer need to establish complex surrogate models which are also unable to establish the relationships of PSP in a reversed direction. The relationships between process, structure, and property can be established simply through ML in whichever direction is desired using the available AM data. DNNs for point data and CNNs for distributions and image data were proposed as the specific ML techniques for the proposed DfAM framework. An ankle brace design problem was used to illustrate the application of the proposed framework. DNNs modelled property-structure relationships used for ankle brace design.

Based on the results, it was demonstrated that the property-structure DNN models were significantly more computationally efficient than conventional surrogate models in computing design variable values, given desired property values. The conventional surrogate models (Gaussian process regression models) needed to be inverted using an optimization method to enable design variable calculation. The property-structure DNN models were trained with the same number of data points as the GPR models and proved to be as accurate. This example helps validate the proposed DfAM framework.

The DfAM framework proposed the use of process-structure-property relationships; however, only structure-property and property-structure relationships were investigated in this paper. Thus, more research is needed to extend the models and method for the larger PSP scope. The property-structure relationships modelled using DNNs in this work related stress-strain values to five design variables (2 inputs, 5 outputs). It is an open issue to determine how well more general, larger, and more complex relationships can be modelled using DNNs and CNNs.

6 Acknowledgements

This research was funded by Digital Manufacturing and Design (DManD) Research Center at the Singapore University of Technology and Design supported by the Singapore National Research Foundation.

7 References

Baturynska, I. (2019). Application of Machine Learning Techniques to Predict the Mechanical Properties of Polyamide 2200 (PA12) in Additive Manufacturing. *Applied Sciences*, *9*(6), 1060. doi:10.3390/app9061060

Baturynska, I., Semeniuta, O., & Wang, K. (2019). Application of machine learning methods to improve dimensional accuracy in additive manufacturing. In *Lecture Notes in Electrical Engineering* (Vol. 484, pp. 245–252). Springer Verlag. doi:10.1007/978-981-13-2375-1_31

Chen, H., & Zhao, Y. F. (2015). Learning algorithm based modeling and process parameters recommendation system for Binder Jetting additive manufacturing process. In *Proceedings of the ASME Design Engineering Technical Conference* (Vol. 1A–2015). American Society of Mechanical Engineers (ASME). doi:10.1115/DETC2015-47627

Chen, J., Siegler, S., & Schneck, C. D. (1988). The three-dimensional kinematics and flexibility characteristics of the human ankle and subtalar joint-part II: Flexibility characteristics. *Journal of Biomechanical Engineering*, *110*(4), 374–385. doi:10.1115/1.3108456

Choi, H., McDowell, D. L., Allen, J. K., Rosen, D., & Mistree, F. (2008). An inductive design exploration method for robust multiscale materials design. *Journal of Mechanical Design, Transactions of the ASME*, *130*(3). doi:10.1115/1.2829860

Chowdhury, S., & Anand, S. (2016). Artificial Neural Network Based Geometric Compensation for Thermal Deformation in Additive Manufacturing Processes. In

Volume 3: Joint MSEC-NAMRC Symposia (p. V003T08A006). http://proceedings.asmedigitalcollection.asme.org/proceeding.aspx?doi=10.1115/MSEC2016-8784. Accessed 10 April 2018

Gibson, I., Rosen, D. W., & Stucker, B. (2010). Design for Additive Manufacturing. In *Additive Manufacturing Technologies* (pp. 299–332). Boston, MA: Springer US. doi:10.1007/978-1-4419-1120-9_11

Gu, J., Wang, Z., Kuen, J., Ma, L., Shahroudy, A., Shuai, B., et al. (2018). Recent advances in convolutional neural networks. *Pattern Recognition*, *77*, 354–377. doi:10.1016/j.patcog.2017.10.013

He, K., Zhang, X., Ren, S., & Sun, J. (2015). Delving Deep into Rectifiers: Surpassing Human-Level Performance on ImageNet Classification. In *The IEEE International Conference on Computer Vision (ICCV)* (pp. 1026–1034).

Huang, J., Chen, Q., Jiang, H., Zou, B., Li, L., Liu, J., & Yu, H. (2020). A survey of design methods for material extrusion polymer 3D printing. *Virtual and Physical Prototyping*, *15*(2), 148–162. doi:10.1080/17452759.2019.1708027

Jang, K. I., Chung, H. U., Xu, S., Lee, C. H., Luan, H., Jeong, J., et al. (2015). Soft network composite materials with deterministic and bio-inspired designs. *Nature Communications*, *6*(1), 1–11. doi:10.1038/ncomms7566

Jiang, J., Hu, G., Li, X., Xu, X., Zheng, P., & Stringer, J. (2019). Analysis and prediction of printable bridge length in fused deposition modelling based on back propagation neural network. *Virtual and Physical Prototyping*, *14*(3), 253–266. doi:10.1080/17452759.2019.1576010

Jiang, J., Weng, F., Gao, S., Stringer, J., Xu, X., & Guo, P. (2019). A Support Interface Method for Easy Part Removal in Direct Metal Deposition. *Manufacturing Letters*, *20*, 30–33. doi:10.1016/j.mfglet.2019.04.002

Jiang, J., Xu, X., & Jonathan Stringer. (2019). Effect of Extrusion Temperature on Printable Threshold Overhang in Additive Manufacturing. In *CIRP Manufacturing Systems Conference 2019*. Ljubljana.

Jiang, J., Xu, X., & Stringer, J. (2018a). Support Structures for Additive Manufacturing: A Review. *Journal of Manufacturing and Materials Processing*, *2*(4), 64. doi:10.3390/jmmp2040064

Jiang, J., Xu, X., & Stringer, J. (2018b). A new support strategy for reducing waste in additive

manufacturing. In *The 48th International Conference on Computers and Industrial Engineering (CIE 48)* (pp. 1–7). Auckland.

Jiang, J., Xu, X., & Stringer, J. (2019a). Optimisation of multi-part production in additive manufacturing for reducing support waste. *Virtual and Physical Prototyping*, *14*(3), 219–228. doi:10.1080/17452759.2019.1585555

Jiang, J., Xu, X., & Stringer, J. (2019b). Optimization of Process Planning for Reducing Material Waste in Extrusion Based Additive Manufacturing. *Robotics and Computer-integrated Manufacturing*, *59*, 317–325. doi:10.1016/j.rcim.2019.05.007

Jin, K. H., McCann, M. T., Froustey, E., & Unser, M. (2017). Deep Convolutional Neural Network for Inverse Problems in Imaging. *IEEE Transactions on Image Processing*, *26*(9), 4509–4522. doi:10.1109/TIP.2017.2713099

Khanzadeh, M., Rao, P., Jafari-Marandi, R., Smith, B. K., Tschopp, M. A., & Bian, L. (2018). Quantifying Geometric Accuracy with Unsupervised Machine Learning: Using Self-Organizing Map on Fused Filament Fabrication Additive Manufacturing Parts. *Journal of Manufacturing Science and Engineering, Transactions of the ASME*, *140*(3). doi:10.1115/1.4038598

Kim, S., Rosen, D. W., Witherell, P., & Ko, H. (2019). A Design for Additive Manufacturing Ontology to Support Manufacturability Analysis. *Journal of Computing and Information Science in Engineering*, *19*(4). doi:10.1115/1.4043531

Lao, W., Li, M., Wong, T. N., Tan, M. J., & Tjahjowidodo, T. (2020). Improving surface finish quality in extrusion-based 3D concrete printing using machine learning-based extrudate geometry control. *Virtual and Physical Prototyping*, *0*(0), 1–16. doi:10.1080/17452759.2020.1713580

Li, Z., Zhang, Z., Shi, J., & Wu, D. (2019). Prediction of surface roughness in extrusion-based additive manufacturing with machine learning. *Robotics and Computer-Integrated Manufacturing*, *57*, 488–495. doi:10.1016/j.rcim.2019.01.004

Liu, W., Wang, Z., Liu, X., Zeng, N., Liu, Y., & Alsaadi, F. E. (2017). A survey of deep neural network architectures and their applications. *Neurocomputing*, *234*, 11–26. doi:10.1016/j.neucom.2016.12.038

Lu, Z. L., Li, D. C., Lu, B. H., Zhang, A. F., Zhu, G. X., & Pi, G. (2010). The prediction of the building precision in the Laser Engineered Net Shaping process using advanced networks. *Optics and Lasers in Engineering*, *48*(5), 519–525.

doi:10.1016/j.optlaseng.2010.01.002

Mahapatra, S. S., & Sood, A. K. (2012). Bayesian regularization-based Levenberg-Marquardt neural model combined with BFOA for improving surface finish of FDM processed part. *International Journal of Advanced Manufacturing Technology*, *60*(9–12), 1223–1235. doi:10.1007/s00170-011-3675-x

Malak, R. J., Aughenbaugh, J. M., & Paredis, C. J. J. (2009). Multi-attribute utility analysis in set-based conceptual design. *CAD Computer Aided Design*, *41*(3), 214–227. doi:10.1016/j.cad.2008.06.004

Matthews, J., Klatt, T., Morris, C., Seepersad, C. C., Haberman, M., & Shahan, D. (2016). Hierarchical Design of Negative Stiffness Metamaterials Using a Bayesian Network Classifier1. *Journal of Mechanical Design, Transactions of the ASME*, *138*(4). doi:10.1115/1.4032774

Mohamed, O. A., Masood, S. H., & Bhowmik, J. L. (2017). Influence of processing parameters on creep and recovery behavior of FDM manufactured part using definitive screening design and ANN. *Rapid Prototyping Journal*, *23*(6), 998–1010. doi:10.1108/RPJ-12-2015-0198

Morris, C., Bekker, L., Haberman, M. R., & Seepersad, C. C. (2018). Design exploration of reliably manufacturable materials and structures with applications to negative stiffness metamaterials and microstereolithography1. *Journal of Mechanical Design, Transactions of the ASME*, *140*(11). doi:10.1115/1.4041251

Negi, S., & Sharma, R. K. (2016). Study on shrinkage behaviour of laser sintered PA 3200GF specimens using RSM and ANN. *Rapid Prototyping Journal*, *22*(4), 645–659. doi:10.1108/RPJ-08-2014-0090

Pacheco, J. E., Amon, C. H., & Finger, S. (2003). Bayesian Surrogates Applied to Conceptual Stages of the Engineering Design Process. *Journal of Mechanical Design, Transactions of the ASME, 125*(4), 664–672. doi:10.1115/1.1631580

Rosen, D. W. (2007). Computer-Aided Design for Additive Manufacturing of Cellular Structures. *Computer-Aided Design and Applications*, *4*(5), 585–594. doi:10.1080/16864360.2007.10738493

Rosen, D. W. (2014). Research supporting principles for design for additive manufacturing. *Virtual and Physical Prototyping*, *9*(4), 225–232. doi:10.1080/17452759.2014.951530

Samuel, A. L. (1959). Some Studies in Machine Learning Using the Game of Checkers - IBM

Journals & Magazine. *IBM Journal of Research and Development*, *3*(3), 210–229.

Shahan, D. W., & Seepersad, C. C. (2012). Bayesian network classifiers for set-based collaborative design. *Journal of Mechanical Design, Transactions of the ASME*, *134*(7). doi:10.1115/1.4006323

Siegler, S., Chen, J., & Schneck, C. D. (1988). The three-dimensional kinematics and flexibility characteristics of the human ankle and subtalar joints—part I: Kinematics. *Journal of Biomechanical Engineering*, *110*(4), 364–373. doi:10.1115/1.3108455

Thiele, F., Schuhmacher, S., Schwaller, C., Plüss, S., Rhiner, J., List, R., & Lorenzetti, S. (2018). Restrictions in the Ankle Sagittal- and Frontal-Plane Range of Movement during Simulated Walking with Different Types of Orthoses. *Journal of Functional Morphology and Kinesiology*, *3*(2), 21. doi:10.3390/jfmk3020021

Thompson, M. K., Moroni, G., Vaneker, T., Fadel, G., Campbell, R. I., Gibson, I., et al. (2016). Design for Additive Manufacturing: Trends, opportunities, considerations, and constraints. *CIRP Annals - Manufacturing Technology*, *65*(2), 737–760. doi:10.1016/j.cirp.2016.05.004

Tootooni, M. S., Dsouza, A., Donovan, R., Rao, P. K., Kong, Z. J., & Borgesen, P. (2017). Classifying the Dimensional Variation in Additive Manufactured Parts from Laser-Scanned Three-Dimensional Point Cloud Data Using Machine Learning Approaches. *Journal of Manufacturing Science and Engineering, Transactions of the ASME*, *139*(9). doi:10.1115/1.4036641

Unal, M., Miller, S. W., Chhabra, J. P. S., Warn, G. P., Yukish, M. A., & Simpson, T. W. (2017). A sequential decision process for the system-level design of structural frames. *Structural and Multidisciplinary Optimization*, *56*(5), 991–1011. doi:10.1007/s00158-017-1697-1

Vijayaraghavan, V., Garg, A., Lam, J. S. L., Panda, B., & Mahapatra, S. S. (2015). Process characterisation of 3D-printed FDM components using improved evolutionary computational approach. *International Journal of Advanced Manufacturing Technology*, *78*(5–8), 781–793. doi:10.1007/s00170-014-6679-5

Wei, H., Shirinzadeh, B., Niu, X., Zhang, J., Li, W., & Simeone, A. (2020). Study of the hinge thickness deviation for a 316L parallelogram flexure mechanism fabricated via selective laser melting. *Journal of Intelligent Manufacturing*. doi:10.1007/s10845-020-01621-x

Weiss, L. E., Amon, C. H., Finger, S., Miller, E. D., Romero, D., Verdinelli, I., et al. (2005). Bayesian computer-aided experimental design of heterogeneous scaffolds for tissue engineering. *CAD Computer Aided Design*, *37*(11), 1127–1139. doi:10.1016/j.cad.2005.02.004

Xiong, J., Zhang, G., Hu, J., & Wu, L. (2014). Bead geometry prediction for robotic GMAW-based rapid manufacturing through a neural network and a second-order regression analysis. *Journal of Intelligent Manufacturing*, *25*(1), 157–163. doi:10.1007/s10845-012-0682-1

Xiong, J., Zhang, Y., & Pi, Y. (2020). Control of deposition height in WAAM using visual inspection of previous and current layers. *Journal of Intelligent Manufacturing*. doi:10.1007/s10845-020-01634-6

Xiong, Y., Duong, P. L. T., Wang, D., Park, S. I., Ge, Q., Raghavan, N., & Rosen, D. W. (2019). Data-driven design space exploration and exploitation for design for additive manufacturing. *Journal of Mechanical Design, Transactions of the ASME*, *141*(10). doi:10.1115/1.4043587

Zhang, W., Mehta, A., Desai, P. S., & Fred Higgs III, C. (2017). Machine Learning Enabled Powder Spreading Process Map for Metal Additive Manufacturing (AM). In *Solid Freeform Fabrication 2017: Proceedings of the 28th Annual International Solid Freeform Fabrication Symposium* (pp. 1235–1249).

Zhao, Y., Sun, J., Gupta, M. M., Moody, W., Laverty, W. H., & Zhang, W. (2017). Developing a mapping from affective words to design parameters for affective design of apparel products. *Textile Research Journal*, *87*(18), 2224–2232. doi:10.1177/0040517516669072